Chiral effects in normal and superconducting carbon nanotube-based nanostructures

A. V. Parafilo[a)]

B. Verkin Institute for Low Temperature Physics and Engineering of the National Academy of Sciences of Ukraine, 47 Lenin Ave., Kharkov 61103, Ukraine

I. V. Krive

B. Verkin Institute for Low Temperature Physics and Engineering of the National Academy of Sciences of Ukraine, 47 Lenin Ave., Kharkov 61103, Ukraine, Department of Physics, University of Gothenburg, Göteborg SE-412 96, Sweden, and Physics Department, V. N. Karazin National University, Kharkov 61077, Ukraine

E. N. Bogachek and U. Landman

School of Physics, Georgia Institute of Technology, Atlanta, Georgia 30332-0430, USA

R. I. Shekhter

Department of Physics, University of Gothenburg, Göteborg SE-412 96, Sweden

M. Jonson

Department of Physics, University of Gothenburg, Göteborg SE-412 96, Sweden, School of Engineering and Physical Sciences, Heriot-Watt University, Edinburgh EH14 4AS, Scotland, United Kingdom, and Division of Quantum Phases and Devices, School of Physics, Konkuk University, Seoul 143-701, Korea

(Submitted May 6, 2010)
Fiz. Nizk. Temp. **36**, 1193–1203 (October–November 2010)

The novel phenomenon of chiral tunneling in metallic single-wall carbon nanotubes is considered. It is induced by the interplay of electrostatic and pseudomagnetic effects in electron scattering in chiral nanotubes and is characterized by an oscillatory dependence of the electron transmission probability on the nanotube chiral angle and the strength of the scattering potential. The appearance of a special (Aharonov–Bohm-like) phase in chiral tunneling affects various phase-coherent phenomena in nanostructures. We examine chiral effects in: (i) persistent currents in circular nanotubes, (ii) Josephson currents in nanotube-based SNS junctions, and (iii) resonant electron tunneling through chiral nanotube-based quantum dots. © *2010 American Institute of Physics*. [doi:10.1063/1.3518334]

I. INTRODUCTION

One of the most spectacular phenomena in physics is the Aharonov–Bohm (AB) effect which was predicted in 1959[1] and realized experimentally a year later.[2] (See also the review by Olariu and Popescu[3] and references therein). This effect is fundamental, it has a simple theoretical formulation, and it has numerous theoretical and experimental applications. This last point concerns, first of all, condensed matter physics where the AB effect is a key idea in a vast number of theoretical and experimental papers.

One of the first and most significant papers on the AB effect in condensed matter physics is a paper by Kulik on non-decaying electric currents in normal metal systems published in 1970.[4] There he predicted that a perfect (impurity-free) small metallic cylinder threaded by magnetic field will support a nondissipative (persistent) electric current with the period equal to a single-flux quantum $\Phi_0=hc/e$[5,6] and an amplitude (at low temperatures) given by the single electron current $\sim ev_F/L$ times the number of transverse channels for a few-channel ring (here v_F is the Fermi velocity and L is the ring circumference). At that time, 15 years before the advent of mesoscopic physics, the prediction that certain physical characteristics of a real many-body (macroscopic) system (now it is better to say mesoscopic) could be sensitive to a single-electron contribution sounded bizarre to many physicists. Although the fundamental nature of Kulik's prediction was evident (the paper was published in the most prestigious physics journal in the Soviet Union), the prospects for experimental observation of this effect seemed obscure. Nevertheless, rather soon the prediction was confirmed, at first in indirect experiments[7,8] with massive cylinders where AB persistent currents were induced by electronic states localized near the surface (whispering gallery states) and forming effectively a doubly connected (ring) geometry.[9,10] Later, in the beginning of the 1990's, persistent currents were measured in a single metallic (gold) ring[11] (diffusive electron transport[12]) and soon thereafter in a quantum ring formed in a 2D electron gas (EG).[13] In a 2DEG, electron transport is ballistic and the measurements[13] were in good agreement with Kulik's prediction.[4]

Since that time persistent currents have been a hot topic in condensed matter physics and there is a vast literature on the problem.[14–17] Aharonov–Bohm oscillations have been observed in metallic rings and cylinders, but also in more exotic systems such as conducting quasi-1D materials with charge density wave excitations,[18] where the AB effect is induced by the quantum coherent dynamics of collective modes.[19,20] Theoretical studies of nontraditional AB effects

 © 2010 American Institute of Physics

Downloaded 22 Jan 2011 to 130.207.50.192. Redistribution subject to AIP license or copyright; see http://ltp.aip.org/about/rights_and_permissions

in condensed matter range from the calculation of persistent currents in dielectrics[21] to the study of AB oscillations induced by superconducting plasmons.[22]

Here we discuss persistent currents in circular carbon nanotubes and supercurrents in nanotube-based superconductor/normal metal/superconductor (SNS) junctions. Both structures have been studied experimentally. Ring-shaped nanotubes (including rings of single-wall nanotubes) have been observed and investigated in Refs. 23 and 24, while measurements of the Josephson current in a single-wall nanotube-based SNS junction have been reported in Ref. 25.

What is distinctive about the transport properties of carbon nanotube-based mesoscopic structures compared to "ordinary" metallic nanowires? Electron transport in metallic single-wall nanotubes (SWNT) is ballistic and this property is explained by a specific scattering of charge carriers by the nanotube defects.[26] Conduction electrons in SWNT are Dirac-like particles and their relativistic spectrum leads to certain peculiarities in electron scattering. In particular, long-range electrostatic potentials in metallic nanotubes do not scatter electrons at all. This effect is explained by the conservation of helicity for relativistic particles. In quantum field theory the phenomenon of particle free penetration through potential barriers is known as the Klein paradox.[27] The specific features of electron scattering in chiral nanotubes and their influence on persistent and super-currents in carbon nanotube-based devices are the subject of the this paper.

In Sec. II we introduce the new concept of chiral tunneling in metallic SWNTs. The transmission and reflection amplitudes are derived for a special 2×2-matrix scattering potential. It is shown that, in the local limit, the transmission coefficient $D(\theta)$ is an oscillating function of the *chiral phase* $\varphi_c = U_0 \cos\theta$, where U_0 is the dimensionless strength of the scattering potential and θ is the nanotube chiral angle. Resonant chiral tunneling, $D_r(\theta)=0$, occurs for quantized values of the chiral phase, with $\varphi_c = \pi n$ (where n is an integer).

In Sec. III we evaluate the persistent current in a circular metallic SWNT with chiral tunneling. We show that the chiral phase φ_c plays a crucial role in the magnetic response of circular carbon nanotubes. In particular, the parity of the chiral resonance (even or odd n) determines the character of the magnetic response (paramagnetic or diamagnetic persistent current). The existence of non-equilibrium spontaneous persistent currents in an isolated nanotube ring with asymmetric populations of the $\pm k_F$-valleys is briefly discussed.

In Sec. IV we consider the influence of chiral effects on the supercurrent in a SWNT-based SNS junction. An equation for the bound state energies (Andreev–Kulik levels) in the presence of chiral tunneling is derived. It is shown that, for energy independent phase factors (forward and backward scattering phases and the chiral phase), the spectral equation expressed in terms of scattering data coincides with the corresponding equation for standard SNS junctions. All information specific to chiral tunneling is hidden in the oscillatory dependence of the junction transparency on the chiral angle and chiral phase. In particular we discuss here the interesting possibility of fabricating highly transparent junctions by using high quality carbon nanotubes with small chiral angles.

In Sec. V, resonant electron transport through a "chiral" quantum dot (QD) (i.e., a QD based on a chiral metallic SWNT) is discussed. We show that when a chiral scatterer exists inside the tube, the spacings between the resonant conductance peaks (measured by varying the gate voltage) depend strongly on the nanotube chiral angle and the chiral phase (which in principle can be regarded as a controllable parameter). The distribution of the number of conductance maxima over level spacing ranges from δ-function like peaks for armchair nanotubes (equidistant spectrum of QD energy levels) to a smooth Wigner-Dysonlike distribution (quasi-random energy spectrum) in chiral nanotubes in the limit of weak chiral tunneling ($D \ll 1$).

In the Conclusion we summarize the main results and briefly discuss the influence of electron-electron interactions on chiral tunneling.

II. CHIRAL TUNNELING

We evaluate the transmission probability for electron scattering by special defects (see below) in carbon nanotubes. We assume that the defect potentials are long-range and do not induce inter-valley electron scattering (δk $\ll$ 2kF). Thus, in our model, the metallic SWNT Hamiltonian is diagonal in the valley index $j=\pm$ and takes the form[28]

$$H_{\pm} = \pm \hbar v_F \begin{pmatrix} 0 & \exp(\pm i\theta)\hat{p}_x \\ \exp(\mp i\theta)\hat{p}_x & 0 \end{pmatrix}. \qquad (1)$$

Here v_F is the Fermi velocity, $\hat{p}_x = -i\partial_x$, θ is the chiral angle of the nanotube ($0 \leqslant \theta \leqslant \pi/6$), and the x-axis is directed along the cylinder axis. Notice that we follow Ref. 28 in the definition of chiral angle ($\theta=0$ for an armchair nanotube and $\theta=\pi/6$ for a zigzag nanotube), which is different from the definition used in Refs. 29 and 30. The presence of chiral factors $\exp(\pm\theta)$ in the Hamiltonian of Eq. (1) results in special scattering of electrons by a non-diagonal potential,[28] an effect which we refer to as *chiral tunneling* in the following.

The electrostatic (scalar) potential is diagonal in the pseudospin indices and cannot induce electron backscattering in our model Eq. (1) owing to the conservation of helicity for massless Dirac particles (the Klein paradox). To get nontrivial scattering of chiral particles we consider the matrix potential

$$\hat{V}_s(x) = \begin{pmatrix} V(x) & V(x) \\ V(x) & V(X) \end{pmatrix}, \qquad (2)$$

which mixes the sublattice components of the electron wave function. For simplicity we consider all matrix elements to be real and equal. An effective scattering potential of the form (2) was suggested in Ref. 28 for electron scattering in metallic carbon nano-peapods. It is induced by hybridization of fullerene molecular orbitals (LUMO) with the conduction electron states in the nanotube.

To proceed further we assume that the scattering potential (2) is "local." However, we cannot take the spatial dependence of $V_s(x)$ to be simply $\delta(x)$. This is because a δ-function scattering potential is ill-defined in the context of the 1D Dirac equation. One has additionally to define the value of the fermion wave function at the singular point x

Downloaded 22 Jan 2011 to 130.207.50.192. Redistribution subject to AIP license or copyright; see http://ltp.aip.org/about/rights_and_permissions

$=0$ (the wave function has a jump at this point). In order to correctly solve the problem, we first consider a rectangular potential of width a and height V_0, which yields an analytical solution for the scattering problem. Then we consider the local scatterer limit by letting $a\to 0$, and $V_0\to\infty$ while keeping the product $V_0 a$ constant.

The transmission and reflection amplitudes for the rectangular potential are found by matching the plane wave and evanescent mode solutions of the Dirac equation at the points $x=0$, a. The transmission amplitude, for instance, takes the form

$$t(E)=\frac{1}{2i\kappa\hbar v_F}\frac{\exp\{i[2\theta-a(k+q)]\}(V_0-E)}{[(V_0-E)^2+\hbar^2v_F^2(\kappa^2-q^2)+V_0e^{i\theta}(2q\hbar v_F-V_0e^{i\theta}\sin a\kappa)]\sin a\kappa-2i\hbar v_F(V_0-E)\kappa\cos a\kappa}, \tag{3}$$

where $\kappa=\sqrt{V_0^2\cos^2\theta-2EV_0+E^2}/\hbar v_F$, $q=V_0\cos\theta/\hbar v_F$, $k=E/\hbar v_F$.

In the limit of interest, Eq. (3) simplifies greatly. The corresponding transmission and reflection amplitudes are

$$t=\frac{\cos\theta\exp(-iU_0\cos\theta)}{\cos\theta\cos(U_0\cos\theta)+i\sin(U_0\cos\theta)},$$

$$r=-\frac{\sin\theta\sin(U_0\cos\theta)}{\cos\theta\cos(U_0\cos\theta)+i\sin(U_0\cos\theta)}. \tag{4}$$

From Eq. (4) we get expressions for the scattering data which will be used below (i.e., for the transmission coefficient $D=tt^*$, and the forward, δ_f, and backward, δ_b, scattering phases)

$$D(\theta)=\frac{\cos^2\theta}{\cos^2(U_0\cos\theta)\cos^2\theta+\sin^2(U_0\cos\theta)},$$

$$R(\theta)=1-D(\theta); \tag{5}$$

$$\delta_f(\theta)=\arctan\left[\frac{\sin(2U_0\cos\theta)\cos^2(\theta/2)}{\cos^2(U_0\cos\theta)\cos\theta-\sin^2(U_0\cos\theta)}\right]$$
$$=U_0\cos\theta+\delta_b(\theta),$$

$$\delta_b(\theta)=\arctan\left[\frac{\tan(U_0\cos\theta)}{\cos\theta}\right]. \tag{6}$$

Here $U_0=aV_o/\hbar v_F$ is the dimensionless strength of the "local" scattering potential in our model. Notice that, after a change of notation, the formula for the transmission coefficient D is the same as the analogous expression for the transmission coefficient in graphene.[31] In our case, the chiral angle θ plays the role of the incident angle of a particle scattered by a rectangular barrier in 2D graphene.

To understand why the quantity $U_0\cos\theta$ appears in the arguments of some of the trigonometric functions, it is useful to find the spectrum of the Dirac equation for the constant matrix potential

$$\hat{V}_s=\begin{pmatrix}V_d & V_o\\ V_o^* & V_d\end{pmatrix}. \tag{7}$$

From Eqs. (1) and (7) we immediately get the spectrum

$$E=V_d\pm\hbar v_F\sqrt{[p+\tilde{U}_0\cos(\theta-\alpha)]^2+\tilde{U}_0^2\sin^2(\theta-\alpha)}, \tag{8}$$

where $\tilde{U}_0\equiv|V_o|/\hbar v_F$ and $V_o=|V_o|\exp(i\alpha)$. We see that the only effect of the diagonal potential V_d is a constant shift of the energy spectrum. The off-diagonal potential V_o (i) induces a gap (if $\theta\neq\alpha$), which mixes left- and rightward moving components of the wave function (i.e., it leads to backscattering events), and (ii) plays the role of a "vector" potential by shifting the momentum to $p+U_o\cos(\theta-\alpha)$. Notice that the potential Vo has to be odd with respect to time reversal ($t\to -t$). Both properties are crucial for chiral tunneling. We will see in the next section that the quantity $U_0\cos\theta$ (we consider real potentials) changes the Aharonov–Bohm phase in the problem of persistent currents. For convenience, we refer to $\phi_c(\theta)=(U_0/2\pi)\cos\theta$ as the dimensionless *chiral flux*.

It is readily seen from Eqs. (5) and (6) that for an armchair ($\theta=0$) nanotube, $D(0)=1$, irrespective of the potential strength; this is an illustration of the Klein paradox in nonchiral metallic nanotubes. In addition, $D(\theta)=1$ for $U_0\cos\theta=\pi N$ (N an integer). The minimum transmission probability, $D_{\min}=\cos^2\theta$, is reached at $U_0\cos\theta=\pi(N+1/2)$. We will refer to these cases as on- and off-resonance chiral tunneling. The "quantization conditions" considered above[31] are typical for quantum resonant transport (see, e.g., Refs. 32 and 33, where an analogous formula for the transmission coefficient is obtained for resonant heat transport through a Luttinger liquid constriction). The on- and off-resonance conditions for chiral tunneling are analogous to the corresponding conditions of constructive ($\Phi/\Phi_0=N$, where Φ is the magnetic flux and $\Phi_0=hc/e$ is the flux quantum) and destructive ($\Phi/\Phi_0=N+1/2$) interference for an Aharonov–Bohm interferometer (see, e.g., Eq. (4.25) of Ref. 34). It is worth noting that, unlike in other resonant scattering problems, it is the potential strength (and not the energy of bound states) which is quantized in our case. The dependences of the transmission coefficient and scattering phases on the chiral angle for different values of the potential are illustrated in Fig. 1.

III. PERSISTENT CURRENTS IN CHIRAL NANOTUBES

A number of theoretical studies of persistent currents in ring-shaped SWNTs have been published. They mostly deal with impurity-free nanotubes and the reported results con-

Downloaded 22 Jan 2011 to 130.207.50.192. Redistribution subject to AIP license or copyright; see http://ltp.aip.org/about/rights_and_permissions

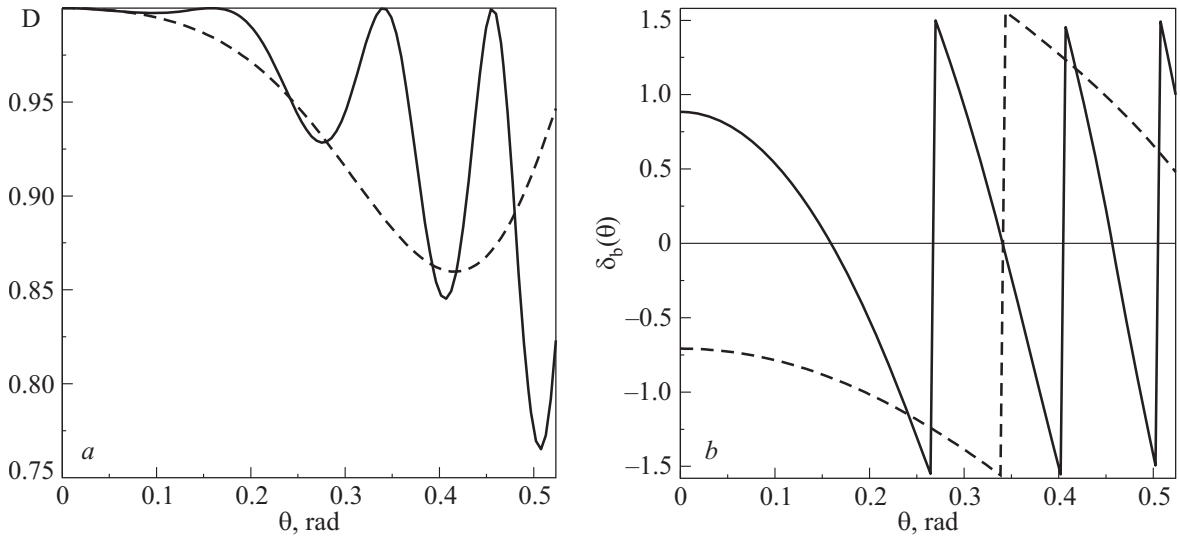

FIG. 1. Transmission coefficient (a) and backward scattering phase (b) as a function of chiral angle at different values of potential strength U0: the solid curve corresponds to $U_0=70$, the dashed curve, to $U_0=15$.

cern specific properties of fullerene toroids,[35] differences in magnetic response of metallic and small gap semiconducting nanotubes,[36] and the influence of electron-electron interactions on persistent currents in defect-free SWNTs.[37] The presence of a short-range scatterer which induces inter-valley electron backscattering ($\delta k \simeq 2k_F$) in sufficiently long nanotubes can be described by a Luttinger liquid model (for a short range electron-electron interaction) or a Wigner crystal model (for an unscreened Coulomb interaction). Persistent currents have been evaluated using these models.[16,38,39] In all these cases the nanotube chirality had no effect on the persistent currents. In this section we consider long-range ("soft") defects which can induce only intra-valley electron scattering. For these processes chiral effects are significant and will determine the properties of the persistent current.

The Hamiltonian of the nanotube in our model is $H=H_j+\hat{V}_s(x)$ where $H_\pm$ and $\hat{V}_s(x)$ are given by Eqs. (1) and (2). We model the spatial dependence of the scattering potential with a rectangular barrier in the local limit (see the previous section). By placing the scatterer at some specific point ($x=a$) we obtain two sets of plane wave solutions of the Dirac equation, one to the left (l) and one to the right (r) of the scatterer. For the "+-valley" they are as follows ($j=l,r$)

$$\Psi_j=\begin{pmatrix}\exp(ik_Fx)[A_j\exp(ikx)+B_j\exp(-ikx)]\\ \exp[i(k_Fx-\theta)][A_j\exp(ikx)-B_j\exp(-ikx)]\end{pmatrix}. \tag{9}$$

The coefficients A_j, B_j are found from two pairs of equations. The first pair,

$$\Psi_r(x+L)=\exp\left(2\pi i\frac{\Phi}{\Phi_0}\right)\Psi_l(x), \tag{10}$$

represents the Aharonov–Bohm boundary condition (L is the ring circumference, $\Phi_0=hc/e$ is the quantum of flux, and we note that, with no scatterers $\Psi_l(x)\equiv\Psi_r(x)$, so that in this case Eq. (10) is the familiar twisted boundary condition for a particle on a ring threaded by a magnetic field). The second pair of equations relates the amplitudes $\Psi_l(a)$ and $\Psi_r(a)$ induced by local potential scattering. It can be written in the form (see the previous section)

$$\begin{pmatrix}A_l\\ B_l\end{pmatrix}=\begin{pmatrix}\frac{1}{t} & \frac{r}{t}\\ \frac{r}{t} & \frac{\exp(i2\pi\phi_c)}{t^*}\end{pmatrix}\begin{pmatrix}A_r\\ B_r\end{pmatrix}, \tag{11}$$

where t and r are the transmission and reflection amplitudes defined in Eq. (4) and $\varphi_c=(U_0/2\pi)\cos\theta$ is the chiral flux. Note that the matrix $\hat{A}$ in Eq. (11) is not a transfer matrix (in particular $\det\hat{A}=\exp(i2U_0\cos\theta)\neq 1$ for $U_0\neq 0$). In our case, the scattering is a two-channel process (we have an additional spinor index) and the corresponding transfer matrix is 4×4-matrix. It is easy to check that the Dirac current is conserved in the scattering process. An analogous set of equations describes the scattering of electrons in the $-k_F$-valley.

The solvability condition for the above linear equations results in the spectral equation

$$\sqrt{D(\theta)}\cos\left(2\pi\frac{\Phi}{\Phi_0}\mp k_FL\pm U_0\cos\theta\right)=\cos[kL-\delta_b(\theta)], \tag{12}$$

where $D(\theta)$ and $\delta_b(\theta)=\delta_f(\theta)-U_0\cos\theta$ are given by Eqs. (5) and (6). Here the upper (lower) signs correspond to the energy spectrum in the $+k_F$-valley ($-k_F$-valley). The term k_FL results in a statistical flux ("parity effects"[40]) in the persistent current of an isolated ring (where the total number of particles is fixed). Chiral tunneling introduces an additional term $\pm U_0\cos\theta$, which have designated as the "chiral phase" φ_c (or chiral flux $\varphi_c=\varphi_c/2\pi$). Note that particles in ($\pm$)-valleys sense chiral fluxes of opposite signs (the l.h.s. of Eq. (12)).

In the limiting case of a local scatterer of interest to us, neither the transmission probability nor the scattering phases depend on energy. So the energy ($E=\pm\hbar v_Fk$) spectrum is given by

Downloaded 22 Jan 2011 to 130.207.50.192. Redistribution subject to AIP license or copyright; see http://ltp.aip.org/about/rights_and_permissions

$$E_{n,j}=\frac{\hbar v_F}{L}\left\{\pm\arccos\left[\sqrt{D(\theta)}\cos\left(2\pi\frac{\Phi}{\Phi_0}-j\varphi_{\text{eff}}\right)\right]+\delta_b(\theta)+2\pi n\right\}, \tag{13}$$

where $n=0,\pm1,\pm2,\ldots,j=\pm$, and $\varphi_{\text{eff}}=k_FL-U_0\cos\theta$ is the effective dimensionless flux. Evaluating the persistent current for a ring at given chemical potential μ,

$$J(\Phi;\theta)=-c\frac{\partial\Omega}{\partial\Phi} \tag{14}$$

(where Ω is the grand canonical thermodynamic potential), for the spectrum given by Eq. (13) is straightforward. The result for a finite temperature T is (we consider here spinless electrons)

$$J=\frac{2}{\pi}I_0\frac{T}{T_*}\sum_{j=\pm,k=1}^{\infty}\frac{\sin\left(2\pi\frac{\Phi}{\Phi_0}+j\varphi_{\text{eff}}\right)}{\sqrt{D^{-1}(\theta)-\cos^2\left(2\pi\frac{\Phi}{\Phi_0}+j\varphi_{\text{eff}}\right)}}\times\frac{\sin\left\{k\arccos\left[\sqrt{D(\theta)}\cos\left(2\pi\frac{\Phi}{\Phi_0}+j\varphi_{\text{eff}}\right)\right]\right\}\cos k\delta(\mu,\theta)}{\sinh\left(k\frac{T}{T_*}\right)} \tag{15}$$

Here $I_0=ev_F/L$, $T_*=\hbar v_F/\pi L$, and $\delta(\mu,\theta)=\mu L/\hbar v_F-\delta_b(\theta)$. We see from Eq. (15) that there is a *spontaneous* persistent current (i.e., at zero external magnetic flux $\Phi=0$; see the discussion in Ref. 17) in each valley. However, at equilibrium and for a ring with a fixed chemical potential, for which the energy levels in the two valleys are equally populated, the net persistent current at zero flux vanishes, $J(\Phi=0;\theta)=0$. This conclusion is, of course, a consequence of the time-reversal invariance of our problem in the absence of an external magnetic field.

The influence of temperature on the persistent current in SWNTs is standard—at high temperatures ($T\gg T_*$) the amplitude of Aharonov–Bohm oscillations is exponentially small. The crossover temperature T_* is determined by the level spacing. Here we consider the low temperature limit $T\ll T_*$ and the case of zero chemical potential, which corresponds to undoped nanotubes. The most interesting situation is that of resonant chiral tunneling ($D=1$, $\delta_b^{\text{res}}=0$). Then persistent current is given by

$$J_{\text{res}}=\frac{8}{\pi}\frac{ev_F}{L}\sum_{k=1}^{\infty}\frac{\sin\left(2\pi k\frac{\Phi}{\Phi_0}\right)}{k}\cos\left[k\pi\left(\frac{N}{2}-n_0\right)\right], \tag{16}$$

where N is the total number of spin-1/2 electrons in the ring (in the half-filled conduction band) and $n_0=U_0\cos\theta/\pi$. As can be readily seen from Eq. (16), the current at $\Phi\neq0$ persists even at the Dirac point ($\mu=0$). In an undoped SWNT ring ($\mu=0$) the total number of particles with energy $E\leqslant0$ and momentum $-k_F<k<+k_F$ is $N=4(m+2)$ (m is an integer). A degeneracy factor of 4 comes from spin$\times$helicity degeneracy and another factor of 2 comes from the double degeneracy of zero-energy modes at each Dirac point. We see that in the absence of chiral tunneling ($U_0=0$) the persistent current is always paramagnetic.[37] Now the response of the ring to a magnetic field depends on the parity of the chiral resonance: for even n_0 the persistent current is paramagnetic, for odd n_0 we have a diamagnetic persistent current.

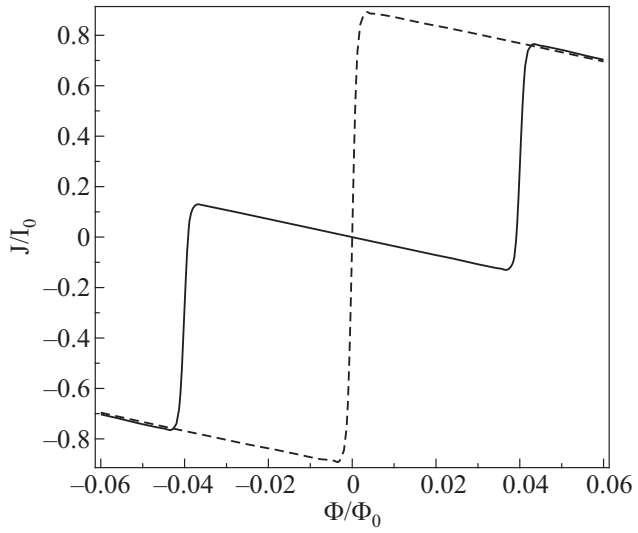

FIG. 2. Persistent current as a function of magnetic flux for different values of the chiral angle near the off-resonance point ($\varphi_c=\pi(n_0+1/2)$; $\theta=0.402$ rad and $U_0=70$ results in $n_0=20$ (this integer represents the 20-th off-resonance point counted from $\theta=\pi/2$ in $D(\theta)$): the solid curve corresponds to $\theta=0.398$ rad, the dashed curve to $\theta=0.418$ rad.

At low temperatures, $T\to0$, and for $\mu=0$, in the off-resonance case ($U_0\cos\theta\to\pi(n_0+1/2)$) the persistent current even for a zigzag nanotube (maximal backscattering coefficient $R=1/4$) is highly anharmonic (it has a prominent sawtooth-like shape). Depending on the parity of n_0 and the approach to the off-resonance point, the current is either paramagnetic (even n_0, from the "left" of the off-resonance point) or diamagnetic (even n_0, from the "right" of the off-resonance point) and vice versa (see Fig. 2). The change from a para- to a diamagnetic response is associated with a jump in the backscattering phase Eq. (6) by $\Delta\delta_b=\pi$ each time the off-resonance condition is passed. Thus, the parity of the resonance (n_0) determines the type of the response up to the off-resonance point, where it changes "smoothly" (see Fig. 2).

In an isolated ring (with a fixed total number of particles) at $T=0$ the population of zero-energy modes can be asymmetric. Then the ring will support a spontaneous persistent current (the sign of the current, clockwise or counterclockwise, will be determined by the specific choice of zero-mode population by chiral electrons). These currents are not equilibrium currents[41] in the presence of even small $2k_F$-backscattering, which tends to symmetrize the population of the zero-energy modes.

IV. CHIRAL EFFECTS ON THE JOSEPHSON CURRENT

We consider the influence of nanotube chirality on the supercurrent through an SNS junction based on a single-wall carbon nanotube. The standard approach for describing S/SWNT/S junctions is to model the normal region as a Luttinger liquid.[42] In Luttinger liquids there are specific phe-

Downloaded 22 Jan 2011 to 130.207.50.192. Redistribution subject to AIP license or copyright; see http://ltp.aip.org/about/rights_and_permissions

nomena (strong enhancement of backscattering off local impurities, spin-charge and charge-entropy separation) which are absent in Fermi liquids. The most important property for charge transport is strong renormalization of the scattering potential by electron-electron interactions, which results in a power-law dependence of the differential conductance on temperature and bias voltage (the Kane-Fisher effect[43]). Backscattering processes ($\delta k \simeq 2k_F$) mix quasiparticles (electrons and holes) of different helicities and the chiral properties of the nanotube cease to be relevant. It is known[44] that in a fully transparent junction (without normal backscattering) the Josephson current is not renormalized by electron-electron interactions. In long SNS tunnel junctions, interactions mostly lead to a renormalization (suppression for repulsive interactions) of the junction transparency.[45,32] In both cases the chirality of the junction does not affect the supercurrent at all.

There is a certain analogy between supercurrents in long SNS junctions ($d \gg \xi_0$, where d is the length of the junction and $\xi_0 = hv_F/\Delta_0$ is the superconducting coherence length) and persistent currents in normal-metal ballistic rings.[46] We have seen already that chiral tunneling leads to new effects in persistent currents. What is the effect of chiral tunneling on the Josephson current through an S/SWNT/S junction?

To calculate the supercurrent in an SNS junction using the equation

$$J = \frac{4e}{\hbar}\frac{\partial \Omega}{\partial \varphi} \tag{17}$$

(where Ω is the thermodynamic potential, φ is the phase difference and the factor 4 counts spin and pseudospin degeneracies), we need to know the spectrum of the Andreev bound states in the normal region (here a SWNT containing a "soft" scatterer). Although we know the scattering characteristics of our potential from Eqs. (5) and (6), we cannot begin by the known formulae for the spectrum of Andreev–Kulik levels[47] and the Josephson current in an SNS junction in terms of the junction transparency. The Andreev scattering in graphene has some peculiarities (specular Andreev reflection)[48] relative to ordinary SNS junctions. Therefore, we shall follow the standard approach and find the spectrum by solving the Bogoliubov-de Gennes (BdG) equation with the order parameter $\Delta(x)$ constant in the superconductors ($\Delta(x) = \Delta_0 e^{i\phi_L}$ for $x<0$, $\Delta(x) = \Delta_0 e^{i\phi_R}$ for $x>d$, where $\varphi_L - \varphi_R = \varphi$) and $\Delta(x) = 0$ in the normal region. The scatterer is placed at the point $x=l$ inside the normal region.

By matching the plane wave solutions of the BdG equation in the normal region at points $x = 0, l, d$ we obtain an equation for the bound state energies (Andreev–Kulik levels[47])

$$\cos\left[\frac{2Ed}{\hbar v_F} - 2\arccos\frac{E}{\Delta_0}\right] = D(\theta)\cos\varphi + R(\theta)\cos\left[\frac{2E(2l-d)}{\hbar v_F}\right], \tag{18}$$

where $R(\theta)$ and $D(\theta)$ are given by Eq. (5). The spectral equation, Eq. (18), is the standard equation for the bound state energies in an SNINS junction (I denotes the scatterer inside the normal region). The phase factor which an electron (hole) acquires during chiral tunneling is energy independent in our model. The phases acquired by electrons and holes are opposite in sign and cancel out in the spectral equation. In addition, as opposed to the problem of persistent currents in a ballistic ring, the effective flux (both statistical and chiral) $\varphi_{\text{eff}} = k_F L - U_0 \cos\theta$ does not enter the spectral equation (18). In the process of Andreev reflection at an S/N boundary, two electrons with small total momentum ($k \ll k_F$) penetrate into the bulk superconductor. This means that an electron in the $+k_F$-valley is reflected as a hole in the $-k_F$-valley (and vice versa). The electron and the hole have opposite momenta and opposite pseudospin (but the same helicity). The two possible helicities (± 1) result in an additional factor 2 in the definition of the Josephson current Eq. (17). We have already seen in the previous section that particles in the different valleys carry effective fluxes φ_{eff} with opposite signs. These contributions to the spectral equation, Eq. (17), cancel out. As a result all information in Eq. (17) specific to SWNTs is hidden in the transmission probability $D(\theta)$. In particular, the nanotube chirality does not influence the Josephson current at all in the absence of normal scattering ($U_0 = 0$).

What, then, are the effects of chiral tunneling on the Josephson current? In chiral nanotubes the junction transparency is an oscillating function of the strength, U_0, of the "soft" scattering potential. Therefore one can expect an anomalous (non-monotonic) behavior of the critical current as a function of potential strength. For resonant chiral tunneling, $U_0 \cos\theta = \pi n_0$, the junction becomes fully transparent ($D_r = 1$) and the supercurrent through an SNINS junction equals (i) the Josephson current through a superconducting constriction (for a short junction $d \ll \xi_0$, where ξ_0 is the superconducting coherence length),[49] $J^{(s)}_{\max}(\varphi) = (2e\Delta/\hbar)\sin(\varphi/2)$ (the additional factor 2 in this formula is due to pseudospin degeneracy), or (ii) the supercurrent through a long, $d \gg \xi_0$, transparent junction $J^{(l)}_{\max}(\varphi) = 2(ev_F/d)(\varphi/\pi)$, where $|\varphi| \leq \pi$. For resonant chiral tunneling the supercurrent does not depend on the position of the scatterer inside the normal region. For off-resonant tunneling the current in a long junction does depend on the actual position ($x=l$) of the local scatterer. However, the effect is numerically small. For the two limiting cases of symmetric ($l = d/2$) and maximally asymmetric ($l = 0, d$) junctions, the supercurrents are

$$J^{\text{off}}_s(\varphi;\theta) = \frac{2}{\pi}\frac{ev_F}{d}\frac{\cos^2\theta\sin\varphi}{\sqrt{1-(\sin^2\theta+\cos^2\theta\cos\varphi)^2}} \times \arccos(\sin^2\theta + \cos^2\theta\cos\varphi), \tag{19}$$

$$J^{\text{off}}_a(\varphi;\theta) = \frac{2}{\pi}\frac{ev_F}{d}\frac{\cos^2\theta\sin\varphi}{\sqrt{(1+\sin^2\theta)^2-\cos^4\theta\cos^2\varphi}} \times \arccos\left(\frac{\cos^2\theta\cos\varphi}{1+\sin^2\theta}\right). \tag{20}$$

The behavior of the supercurrents $J_{s,a}$ for different chiral angles is shown in Fig. 3. We see that for given θ and φ, the current through a symmetric junction is always larger (although the effect is numerically small) than the current through an asymmetric junction.

Downloaded 22 Jan 2011 to 130.207.50.192. Redistribution subject to AIP license or copyright; see http://ltp.aip.org/about/rights_and_permissions

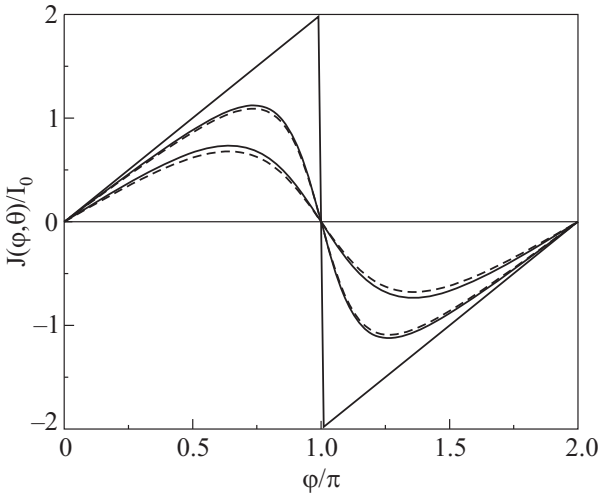

FIG. 3. The Josephson current (in units of $I_0=ev_F/d$) in a long junction, $U_0=70$; the solid curves correspond to the chiral resonance ($\theta=0.158$ rad) and two off-resonance cases $\theta=0.276$ rad and $\theta=0.507$ rad (symmetric junction); the corresponding currents in an asymmetric junction are represented by the dashed curves.

It has been proposed that the pair of Andreev levels in a short SNS junction be used as a qubit ("Andreev qubit," see Ref. 50) and for cooling of nanoelectromechanical devices.[51] In these proposals the coherent dynamics of the Andreev–Kulik levels occur deep inside the gap region ($E \ll \Delta_0$, where Δ_0 is the superconducting order parameter). This regime can be attained only with almost fully transparent junctions, and chiral nanotube-based junctions might be promising candidates for the fabrication of SNS junctions with high transparency $D-1 \ll 1$.

In the general case of non-resonant chiral tunneling, the minimum energy separation between a pair of Andreev–Kulik levels in a short SNS junction is $E_g(\theta)=2\Delta_0\sqrt{1-D(\theta)}$. The minimal junction transparency $D_{\min}=\cos^2\theta$ is reached at $U_0\cos\theta=\pi(n_0+1/2)$ (chiral off-resonance), so the gap

$$E_g(\theta) = 2\Delta_0 \sin\theta \tag{21}$$

could be arbitrarily small for nanotubes with small chiral angles.

V. RESONANT TUNNELING THROUGH A CHIRAL QUANTUM DOT

Resonant electron tunneling in quantum wires[52] is a coherent quantum mechanical phenomenon which is extremely sensitive to the electron energy spectrum. Transport experiments with quantum dots in the resonant tunneling regime (resonant transport spectroscopy) yield valuable information about the electron energies and electron wave functions in the dot by measuring the position and the shape of resonance conductance peaks as functions of the gate voltage. Since their discovery, single-wall carbon nanotubes have been regarded as promising elements for future nanoelectronics. In particular, carbon nanotube-based single electron transistors (SET) have been fabricated and electron transport through these molecular devices has been studied over a wide range of temperatures.[53] The observation at low temperatures of Coulomb blockade oscillations and resonant electron tunneling in long (a few hundred nanometers) metallic SWNTs means that electrons are delocalized along the whole length of the structure. This fact is usually explained by the specifics (Klein paradox) of charge carrier (massless Dirac electrons) scattering in SWNTs by long-range tube defects.[26] Chiral tunneling in this sense has already been indirectly observed in SWNT-based quantum dots. Here we consider the direct influence of chiral tunneling on the resonant transport properties of quantum dots.

We model a "chiral quantum dot" by a finite length (L) metallic chiral SWNT, Eq. (1), with a "soft" local scatterer, Eq. (4), placed at a distance l from the left end of the nanotube. The nanotube is connected to the leads by normal tunnel barriers, which results in a finite (small) width Γ of the electron energy levels (we assume the widths are energy independent). The electron energy spectrum can be found, to lowest order in Γ, by assuming that the end barriers are infinite. The corresponding boundary conditions can be formulated as the absence of any electron (Dirac) current through the ends of the nanotube, i.e., $j_D(x=0,L)=0$. Since scattering at the ends connects electrons in the $+k_F$ and $-k_F$ valleys, the current should be expressed in terms of the 4-spinors $\Psi^T=(\psi_+^T,\psi_-^T)$, where T denotes transposition. For our Hamiltonian, Eq. (1), the current is given by

$$j_D(x) = v_F\Psi^\dagger(x)\begin{pmatrix} 0 & e^{i\theta} & 0 & 0 \\ e^{-i\theta} & 0 & 0 & 0 \\ 0 & 0 & 0 & -e^{-i\theta} \\ 0 & 0 & -e^{i\theta} & 0 \end{pmatrix}\Psi(x). \tag{22}$$

The physically evident solution for these boundary conditions is scattering at the boundaries, with a left-moving fermion in the "+"-valley being transformed into a right-moving fermion in the "−"-valley and all analogous processes following $L^{\pm}\leftrightarrow R^{\mp}$. In general, this scattering is accompanied by an energy-independent phase shift.

By matching the plane wave solutions of the Dirac equation at the points $x=0,l,L$ using our boundary conditions and the matrix Eq. (11) for "+"- and "−"-valleys ($\theta\to-\theta$) we obtain the spectral equation

$$\cos[2kL-\zeta(\theta)] = R(\theta)\cos[2k(L-2l)] + D(\theta)\cos(2k_FL-2U_0\cos\theta), \tag{23}$$

where the total scattering phase $\zeta(\theta)$ is given by

$$\zeta(\theta) = \arctan\left[\frac{\sin(2U_0\cos\theta)\cos\theta}{\cos^2(U_0\cos\theta)\cos^2\theta-\sin^2(U_0\cos\theta)}\right] = 2[\delta_f(\theta)-U_0\cos\theta]. \tag{24}$$

Equation (23) coincides with Eq. (18) of Ref. 54. However, the expressions for the scattering data are different in our case (the assumptions about the scattering potential used to derive the transmission and reflection amplitudes in Ref. 54 are not satisfied in our model). The derived spectral equation has a simple physical interpretation. The phase terms in Eq. (23) depend on: (i) the "quantization length" $2L$ (at the boundaries inter-valley electron scattering occurs and a $2L$-path is necessary to form a closed trajectory), (ii) twice the forward scattering phase $2\delta_f(\theta)$ acquired by a particle as it crosses the scattering potential twice, and (iii) the twice the

Downloaded 22 Jan 2011 to 130.207.50.192. Redistribution subject to AIP license or copyright; see http://ltp.aip.org/about/rights_and_permissions

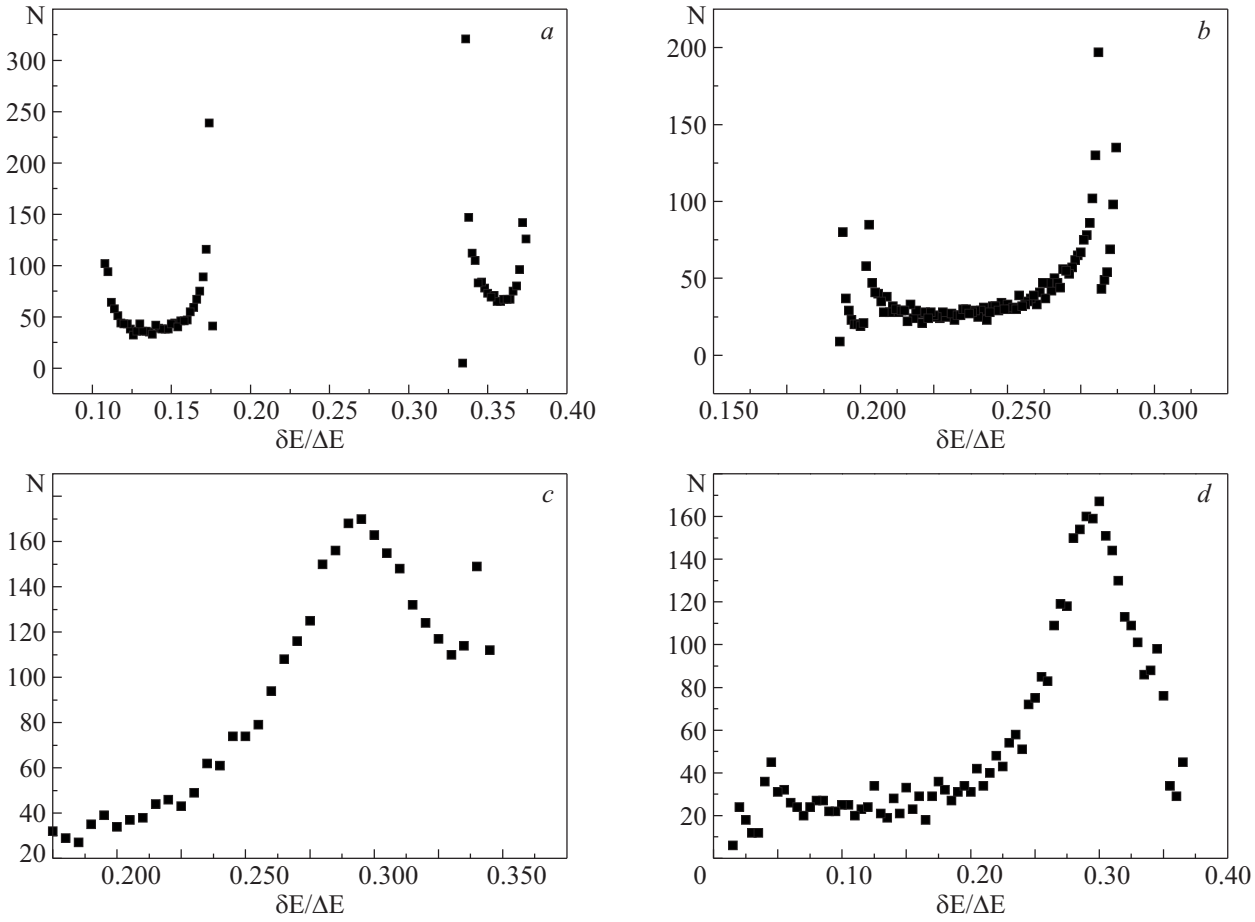

FIG. 4. The distribution of the number of energy levels over the level spacing (normalized by $\Delta E=\pi\hbar v_F/L$) for $U_0=20$ and different chiral angles: to $\theta=0.49$ rad (D=0.8) (a), $\theta=0.52$ rad (D=0.75) (b), $\theta=0.955$ rad (D=0.4) (c), and $\theta\approx\pi/2$ (D=0.06) (d). For the armchair nanotube we have two sets of equidistant energy levels: $\delta E/\Delta E=0.13$ and 0.36. The distribution for $l/L=1/2\pi$ and $\Gamma=0.002$ is shown here.

chiral phase $2U_0\cos\theta=2\varphi_c$, which is added to the geometrical phase $2k_FL$.

Since the momentum k_F is defined for an undoped nanotube it can be expressed in terms of the total number of particles in a half-filled conduction band as $k_FL=\pi N/2$, where $N=4(m+2)$, with m an integer. (See the discussion in Sec. III.) We see that the phase associated with the terms in k_FL does not influence the spectral properties of chiral quantum dots. For armchair nanotubes ($R(0)=0$ and $\delta_f(0)=2U_0+\pi n$ with modulus 2π) the spectral equation reads $\cos(2kL-2U_0)=\pm\cos 2U_0$, which results in two sets of equidistant energy levels ($\Delta E=\pi\hbar v_F/L$) which are shifted relative each other by $\delta_f(0)\hbar v_F/L$. Note that, for $\delta_f\simeq\pi$, the level spacing is approximately halved (this halved level spacing is usually regarded as an averaged level spacing in SWNT). In the case of chiral resonant tunneling, the electron energy spectrum in a chiral nanotube does not depend on the position of the chiral scatterer (as for armchair nanotubes). It is still equidistant with energy spacing $\pi\hbar v_F/L$. In the general case of nonresonant scattering, the energy spectrum is quasi-random for irrational values l/L. The distribution of the number of energy levels over the level spacing (normalized by $\Delta E=\pi\hbar v_F/L$) for a given potential strength and different chiral angles is shown in Fig. 4. Levels with energy differences less then the level width Γ are regarded as "degenerate." We see that two δ-function-like peaks for $\theta=0$ occur with sufficiently strong backscattering ($D\ll 1$) for a distribution which resembles the Wigner–Dyson distribution. Although small transmission coefficients correspond to nonphysical chiral angles (θ close to $\pi/2$) in our model (real potentials Vd and Vo of equal strengths), small transparencies in chiral tunneling could be realized in the general case of nonsymmetric potentials.

With resonant electron tunneling through quantum dots, the distribution of the spaces between the peak (maximum) conductances as a function of gate voltages is determined by the distribution of the level spacings in the electron energy spectrum. We have shown that the mechanism of chiral tunneling is sensitive to the chirality of nanotubes. This phenomenon could, therefore, be used to determine the nanotube chiral angle by resonant transport spectroscopy.

VI. CONCLUSION

In this paper we have introduced the new concept of chiral tunneling in metallic single-wall carbon nanotubes. There are significant differences between the Klein (or chiral) tunneling of massless 2D Dirac-like particles in graphene (well studied in recent years[27]) and chiral tunneling of 1D massless fermions in SWNTs. In the 2D scattering problem for graphene, even a scalar electromagnetic potential can backscatter massless Dirac electrons if the incident angle of a scattering particle is not close to zero (for normal incidence the transmission coefficient is always $D=1$). In a SWNT,

Downloaded 22 Jan 2011 to 130.207.50.192. Redistribution subject to AIP license or copyright; see http://ltp.aip.org/about/rights_and_permissions

scattering is a 1D problem and one can expect a finite reflection probability for massless Dirac particles only in chiral nanotubes in which spiral-like electron "motion" along the cylinder axis mimics some features of 2D scattering. In addition, with nontrivial scattering ($R \neq 0$) the scattering potential cannot be purely electrostatic ("diagonal" in our representation for the Dirac matrices). The presence of nondiagonal components induced by a pseudovector potential (pseudomagnetic effects) are crucial for chiral tunneling in nanotubes. Here we have used a phenomenological approach to the problem and postulated a matrix scattering potential of the form of Eq. (2) in order to study the general properties of chiral tunneling. We know of at least one example where such a matrix potential has been derived microscopically: the effective scattering potential induced by fullerene molecules in nano-peapods.[28] Note that magnetic potentials in nanostructures are, as a rule, long-range and are consistent with our assumption of a "smooth" scattering potential.

We have shown that in chiral tunneling, besides the (small) reflection probability, one of the important physical characteristics which also plays a significant role in the process is the chiral phase, $\varphi_c = U_0 \cos\theta$, a quantity associated with the effective vector potential experienced by the particle in the process of tunneling. It is worth noting that the forward and backward scattering phases in chiral tunneling are related by the simple expression $\delta_f - \delta_b = \varphi_c$. The quantized chiral phase determines the conditions for resonant ($\varphi_c = \pi n$, where n is an integer, and $D_r = 1$) and off-resonant ($\varphi_c = \pi(n+1/2)$, $D_0 = \cos^2\theta$) chiral tunneling.

The chiral phase is added to the magnetic flux in the problem of Aharonov–Bohm oscillations and its appearance can result in a spontaneous persistent current in a ring with an asymmetric population of zero-energy modes. Since particles with opposite helicities acquire chiral phases of opposite signs, the chiral phases are cancelled in the Josephson current problem when a pair of electrons ($-k_F + k_F$) tunnel to the bulk superconductor. We have demonstrated the nontrivial role played by the chiral phase in various phase coherent phenomena in nanostructures.

The last question we would like to discuss here is the influence of electron-electron interactions on chiral tunneling. We assume that the interaction is not strong, otherwise Luttinger liquid effects, which strongly enhance $2k_F$-backscattering, will violate our assumption of a smooth diagonal scattering potential. It is physically evident that, under the conditions of resonant chiral tunneling ($D_r = 1$), electron-electron interactions do not renormalize chiral scattering potentials at all. Off-resonance there is finite backscattering and one could expect its enhancement by (repulsive) interaction effects. This problem merits special consideration. Here we note briefly that, in the limit of weak interactions, when renormalization is induced by electron scattering on Friedel oscillations,[55] the naive mean-field approximation for the interaction potential does not lead to logarithmic infra-red singularities in the backscattering amplitudes.

We gratefully acknowledge discussions with L. Gorelik, A. Kadigrobov, S. Kulinich and V. Shumeiko. AVP thanks V.Yu. Monarkha for help with numerical calculations. This work was supported in part by the Swedish VR, the European Commission (FP7-ICT-2007-C; proj. No. 225955 STELE), and the Korean WCU program funded by MEST through KOSEF (R31-2008-000-10057-0). The research of ENB and UL was supported by the US Department of Energy under Grant No. FG05-86ER45234. IVK acknowledges the hospitality of the Department of Physics at the University of Gothenburg.

[a]Email: krive@ilt.kharkov.ua

[1]Y. Aharonov and D. Bohm, Phys. Rev. **115**, 485 (1959).
[2]R. G. Chambers, Phys. Rev. Lett. **5**, 3 (1960).
[3]S. Olariu and I. I. Popescu, Rev. Mod. Phys. **57**, 339 (1985).
[4]I. O. Kulik, Pis'ma Zh. Eksp. Teor. Fiz. **11**, 407 (1970) [JETP Lett. **11**, 275 (1970)].
[5]L. Gunther and Y. Imry, Solid State Commun. **7**, 1391 (1969).
[6]F. Bloch, Phys. Rev. B **2**, 109 (1970).
[7]N. B. Brandt, D. V. Gitsu, A. A. Nikolaeva, and Ya. G. Ponomarev, Pis'ma Zh. Eksp. Teor. Fiz. **24**, 304 (1976) [JETP **24**, 272 (1976)].
[8]N. B. Brandt, E. N. Bogachek, D. V. Gitsu, G. A. Gogadze, I. O. Kulik, A. A. Nikolaeva, and Ya. G. Ponomarev, Fiz. Nizk. Temp. **8**, 718 (1982) [Sov. J. Low Temp. Phys. **8**, 358 (1982)].
[9]E. N. Bogachek and G. A. Gogadze, Zh. Eksp. Teor. Fiz. **63**, 1839 (1972) [Sov. J. Low Temp. Phys. **36**, 973 (1973)].
[10]E. N. Bogachek, A. G. Scherbakov, and U. Landman, Phys. Rev. B **63**, 115323 (2001).
[11]V. Chandrasekhar, R. A. Webb, M. J. Brady, M. B. Ketchen, W. J. Gallagher, and A. Kleinsasser, Phys. Rev. Lett. **67**, 3578 (1991).
[12]M. Büttiker, Y. Imry, and R. Landauer, Phys. Lett. A **A96**, 365 (1983).
[13]D. Mally, C. Chapelier, and A. Benoit, Phys. Rev. Lett. **70**, 2020 (1993).
[14]Y. Imry, Introduction to Mesoscopic Physics, Oxford Univ. Press (1997).
[15]I. V. Krive and A. S. Rozhavsky, Int. J. Mod. Phys. B **B6**, 1255 (1992).
[16]A. A. Zvyagin and I. V. Krive, Fiz. Nizk. Temp. **21**, 687 (1995) [Low Temp. Phys. **21**, 533 (1995)].
[17]I. O. Kulik, Fiz. Nizk. Temp. **30**, 705 (2004) [Low Temp. Phys. **30**, 528 (2004)].
[18]Y. I. Latyshev, O. Laborde, P. Monceau, and S. Klaumunzer, Phys. Rev. Lett. **78**, 919 (1997).
[19]E. N. Bogachek, I. V. Krive, I. O. Kulik, and A. S. Rozhavsky, Phys. Rev. B **42**, 7614 (1990).
[20]E. N. Bogachek, I. V. Krive, I. O. Kulik, and A. S. Rozhavsky, Zh. Eksp. Teor. Fiz. **97**, 603 (1990) [Sov. J. Low Temp. Phys. **70**, 336 (1990)].
[21]I. O. Kulik, A. S. Rozhavskii, and E. N. Bogachek, JETP Lett. **47**, 303 (1988).
[22]E. N. Bogachek, I. A. Romanovsky, and U. Landman, Phys. Rev. B **78**, 174515 (2008).
[23]J. Liu, H. Dai, J. H. Hafner, D. T. Colbert, R. E. Smalley, S. J. Tans, and C. Dekker, Nature **385**, 780 (1997).
[24]R. Martel, H. R. Shea, and Ph. Avouris, Nature **398**, 299 (1999).
[25]A. Yu. Kasumov, R. Deblock, M. Kociak, B. Reulet, H. Bouchiat, I. I. Khodos, Yu. B. Gorbatov, V. T. Volkov, C. Journet, and M. Burghard, Science **284**, 1508 (1999).
[26]P. L. McEuen, M. Bockrath, D. H. Cobden, Y. G. Yoon, and S. G. Louie, Phys. Rev. Lett. **83**, 5098 (1999).
[27]A. H. C. Neto, F. Guinea, N. M. R. Peres, K. S. Novoselov, and A. K. Geim, Rev. Mod. Phys. **81**, 109 (2009).
[28]C. L. Kane, E. J. Mele, A. T. Johnson, D. E. Luzzi, B. W. Smith, D. J. Hornbaker, and A. Yazdani, Phys. Rev. B **66**, 235423 (2002).
[29]R. Saito, G. Dresselhaus, and M. S. Dresselhaus, Physical Properties of Carbon Nanotubes, Imperial College Press, London (1998).
[30]Carbon Nanotubes: Synthesis, Structure, Properties, and Applications, M. S. Dresselhaus, G. Dresselhaus, and Ph. Avouris (eds.), Top. Appl. Phys. 80, Springer (2001).
[31]M. I. Katsnelson, K. S. Novoselov, and A. K. Geim, Nat. Phys. **2**, 620 (2006).
[32]I. V. Krive, Fiz. Nizk. Temp. **24**, 458 (1998) [Low Temp. Phys. **24**, 377 (1998)].
[33]I. V. Krive, Phys. Rev. B **59**, 12338 (1999).
[34]M. Büttiker, Y. Imry, and M. Ya. Azbel, Phys. Rev. **A30**, 1982 (1984).
[35]R. C. Haddon, Nature **388**, 31 (1997).
[36]M. F. Lin and D. S. Chuu, Phys. Rev. B **57**, 6731 (1998).

Downloaded 22 Jan 2011 to 130.207.50.192. Redistribution subject to AIP license or copyright; see http://ltp.aip.org/about/rights_and_permissions

[37]A. A. Odintsov, W. Smit, and H. Yoshioka, Europhys. Lett. **45**, 598 (1999).
[38]I. V. Krive, P. Sandstrom, R. I. Shekhter, S. M. Girvin, and M. Jonson, Phys. Rev. B **52**, 16451 (1995).
[39]A. O. Gogolin and N. V. Prokofiev, Phys. Rev. B **50**, 4921 (1994).
[40]D. Loss, Phys. Rev. Lett. **69**, 343 (1992).
[41]T. Swahn, E. N. Bogacheck, Y. M. Galperin, M. Jonson, and R. I. Shekhter, Phys. Rev. Lett. **73**, 162 (1994).
[42]I. V. Krive, R. I. Shekhter, and M. Jonson, Fiz. Nizk. Temp. **32**, 1171 (2006) [Low Temp. Phys. **32**, 887 (2006)].
[43]C. L. Kane and M. P. A. Fisher, Phys. Rev. Lett. **68**, 1220 (1992).
[44]D. L. Maslov, M. Stone, P. M. Goldbart, and D. Loss, Phys. Rev. B **53**, 1548 (1996).
[45]R. Fazio, F. W. J. Hekking, and A. A. Odintsov, Phys. Rev. Lett. **74**, 1843 (1995).
[46]I. V. Krive, S. I. Kulinich, R. I. Shekhter, and M. Jonson, Fiz. Nizk. Temp. **30**, 738 (2004) [Low Temp. Phys. **30**, 554 (2004)].
[47]I. O. Kulik, Zh. Eksp. Teor. Fiz. **57**, 1745 (1969) [Sov. J. Low Temp. Phys. **30**, 944 (1970)].
[48]C. W. J. Beenakker, Phys. Rev. Lett. **97**, 067007 (2006).
[49]I. O. Kulik and A. N. Omelyanchouk, Fiz. Nizk. Temp. **3**, 945 (1977) [Sov. J. Low Temp. Phys. **3**, 459 (1977)].
[50]A. Zazunov, V. S. Shumeiko, E. N. Bratus', J. Lantz, and G. Wendin, Phys. Rev. Lett. **90**, 087003 (2003); A. Zazunov, V. S. Shumeiko, E. N. Bratus', and G. Wendin, Phys. Rev. B **71**, 214505 (2005).
[51]G. Sonne, M. E. Peña-Aza, L. Y. Gorelik, R. I. Shekhter, and M. Jonson, *Cooling of a Suspended Nanowire by an AC Josephson Current Flow*, arXiv:1002.1207 (2010).
[52]I. V. Krive, A. Palevski, R. I. Shekhter, and M. Jonson, Fiz. Nizk. Temp. **36**, 155 (2010) [Low Temp. Phys. **36**, 119 (2010)].
[53]J. Nygård, D. H. Cobden, M. Bockrath, P. L. McEuen, and P. E. Lindelöf, Appl. Phys. **A69**, 297 (1999).
[54]I. V. Krive, R. Ferrone, R. I. Shekhter, M. Jonson, P. Utko, and J. Nygård, New J. Phys. **10**, 043043 (2008).
[55]K. A. Matveev, D. Yue, and L. I. Glazman, Phys. Rev. Lett. **71**, 3351 (1993).

This article was published in English in the original Russian journal. Reproduced here with stylistic changes by AIP.

Downloaded 22 Jan 2011 to 130.207.50.192. Redistribution subject to AIP license or copyright; see http://ltp.aip.org/about/rights_and_permissions